World Academy of Science, Engineering and Technology
International Journal of Materials and Metallurgical Engineering
Vol:17, No:10, 2023

Structural and Optical Properties of $CdSiP_2$ and $CdSiAs_2$ Nonlinear Optical Materials

N. N. Omehe

***Abstract*—**$CdSiP_2$ and $CdsiAs_2$ are nonlinear optical materials for near and mid-infrared applications. Density functional theory has been applied to study the structure, band gap, and optical properties of these materials. The pseudopotential method was used in the form of projector augmented wave (PAW) and norm-conserving, the band structure calculations yielded a band gap of 1.55 eV and 0.88 eV for $CdSiP_2$ and $CdsiAs_2$ respectively. The values of $\varepsilon_1(\omega)$ from the doelectric function calculations are 15 and 14.9 $CdSiP_2$ and $CdsiAs_2$ respectively.

***Keywords*—**Band structure, chalcopyrite, near-infrared materials, mid-infrared materials, nonlinear material, optical properties.

I. Introduction

$CdSiP_2$ and $CdSIAS_2$ are nonlinear optical materials with applications in the near and mid infrared region of the electromagnetic spectral. They are ternary chalcopyrite compounds of the form II- IV-V2 and have wide range of applications. They have applications in lasers [1] [2], spintronics and opto-electronic devices [3], solar cells and photocathodes [4]. These materials have been extensively, studied experimentally, though few works have been theoretically.

Isomura and Masumoto [5] were among the first to grow the $CdSiP_2$ crystals, the crystal was grown in Sn metal bath, they reported on its transmission T and reflectivity R. Kaufmann et al. [6] studied the antisite defects in $CdSiP_2$, GAP, and $ZnGeP_2$ using electron spin resonance (ESR). Mughal et al. [7] worked on crystal growth of some ternary compounds including $CdSiP_2$ and reported on their phase matching properties, also, crystals of $CdSiP_2$ were grown by Schunemann et al. [8], and they reported on its phase matching properties. Petrov et al. [9] reported on the nonlinear coefficient d_{36} of $CdSiP_2$, the study was carried out using optical parametric amplifier. Sooriyagoda et al. [10] used the Terahertz time-domain spectroscopy to study the temperature dependence of the refraction and absorption of $CdGeP_2$, ZnGeP2, and $CdSiP_2$. Using the Stoichiometric melt method, Zawilski et al. [11] grew large single crystals of $CdSiP_2$, and measured their optical and thermal properties. Hui et al. [12] grew the crystal of $CdSiP_2$ by the modified vertical Bridgman (VB) method, and reported on the thermal properties of $CdSiP_2$. Wei et al. [13] studied the temperature dependence of the refractive indices ranging from 90K to 450K. Scherrer et al. [14] used the Horizontal Gradient Freeze (HGF) method to grow the crystal of $CdSiP_2$, and carried out analysis by electron parametric resonance, and reported on the optical absorption of $CdSiP_2$.

Komandin et al. [15] studied the Terahertz absorption in $CdSiP_2$ by Backward wave oscillator, time-domain and infrared spectroscopy. Ferdinandus et al. [1] measured the birefringence of $CdSiP_2$ using the Z-scan technique at near and mid-infrared wavelength. They reported that conversion efficiency of $CdSiP_2$ is impacted by absorption. Bereznaga et al. [16] succeeded in growing the crystal of $CdSiP_2$ from its constituent elements, and analyzed it by X-diffraction and scanning electron microscopy with energy-dispersive spectroscopy, they reported on the optical properties. Li et al. [17] used the VB method of crystal growth in growing the $CdSiP_2$ crystal and characterized it using the Terahertz time-domain spectrometer and reported on its conversion efficiency. Carnio et al. [18] reported on the capability of $CdSiP_2$ crystals in detecting electric field waveforms within the high terahertz and infrared spectral.

On the theoretical approach, Chiker et al. [19] investigated the band structure and optical properties of $CdSiP_2$ using the full potential linearized augmented plane wave (FPLAPW) method, and reported a band gap value of 1.1 eV, while Basalaev et al. [20] used the pseudopotential method to study the structure of $MgSiP_2$, $ZnSiP_2$, and $CdSiP_2$. In their work, Xiao et al. [21] employed the HSE06 hybrid functional to study the electronic structure, bonding and optical properties of $CdSiP_2$, and reported a band gap of about 2.0 eV. Hou et al. [22], in their DFT study, reported a band gap of 1.358 eV. Hadda et al. [23] calculated the structural, electronic, optical and elastic parameters of $CdSiX_2$ (X = P, As), a DFT study using GGA, and reported a direct band gap at the gamma point, they also reported on the optical properties of the investigated materials. Jabbar and Reshak [24] used the full potential linearized augmented plane wave (FP-LAPW) method for investigation of the electronic structure and optoelectronic properties of $CdSiP_2$ and reported a band gap of 2.10 eV. The GW method was applied to study structure electronic, optical and vibrational properties of $CdSiP_2$ by Yu et al. [25]. They reported a band gap value of 2.302 eV. The electronic and optical properties of $CdSiAS_2$ have also been reported by Kumavat et al. [26], [27]. Kimmel et al. [28] used the chemical vapor method to grow single crystal of P-doped $CdSiAS_2$. They reported on the photoluminescence of the crystal. Also, Avirovic et al. [29] used the chemical vapor transport method to grow single crystals of $CdSiAS_2$, and for characterization, used X-ray and chemical analysis. The photoluminescence of $CdSiAS_2$ when doped with sulphur was studied by Osinsky et al. [30].

Omehe N. N. is with the Federal University Otuoke, Bayelsa States, Nigeria (phone: +23407031003831; e-mail: omehenn@fuotuoke.edu.ng).

II. Computational Details

Chalcopyrites are tetragonal structure belonging to the space group I-42d with number 122 in crystallographic table. They are superlattice of the zinc-blende structure. In the structure optimization, the Silicon (Si) atoms were assigned the 4a atomic coordinates in the Wyckoff coordinates in the crystallographic table, while the Cadmium (Cd) atoms were assigned the 4b atomic coordinates. The Arsenic (As) and Phosphorus atoms were assigned the 8d coordinates. The structure has four formula unit in a unit cell, that is, a Z value of four. The total number of atoms in the unit cell is 16.

The pseudopotential method as implemented in the Abinit package [31], [32] was used in all computations. The following calculations were carried out in this study: structure optimization, the band structure, density of states, which include the total and partial densities of states, and the optical properties. The structure optimization is the energy minimization with respect to atomic positions and the results are the lattice parameters, the deformation parameter, and the atomic positions; these were then used to calculate the band structure, density of states, and the optical properties. The minimization was done using norm-conserving pseudopotentials. Table I shows the results of the optimization. The LDA+U scheme also implemented in the Abinit package was employed in the electronic band structure and density of state computations. The PAW in conjunction with LDA+U was used in these computations. In the ground state calculations, the tolerance on energy was 10^{-10}, a kinetic cutoff energy of 15 Ha and a shifted grid of 4x4x4 yielding a k-points of 256 points were used. For the optical properties, the norm-conserving pseudopotential and a k-point of 500 was used.

TABLE I
Optimization Result

	Lattice parameter (Å)	Lattice parameter (Exp) Å
$CdSiP_2$	a = 5.641 c = 10.5242	a = 5.679[a] c = 10.431[a]
$CdSiAs_2$	5.955 10.911	5.885[a] 10.881[a]

[a][33]

III. Results Presentation and Discussion

The electronic band structure of cadmium silicon diphosphide ($CdSiP_2$) and cadmium silicon diarsenide ($CdSiAs_2$) are shown in Figs. 1 (a) and (b), respectively. The plot for $CdSiP_2$ is presented in Fig. 1 (a), the plot is energy (eV) against high symmetry points in the first Brillouin zone in the Γ – Z – M – A – Γ – X – R direction. The plot is divided into two windows by the Fermi level, which is indicated at the zero mark by the dashed line. These windows are the conduction band and the valence band. The conduction band minimum (CBM) and the valence band maximum (VBM) both coincide at the gamma (Γ) point of the Brillouin zone. This implies that, the band gap is direct, and the material a semiconductor. The calculated energy band gap for $CdSiP_2$ is 1.55 eV which agreed fairly well with the experimental value of 2.2 eV [33] and other previous works. For $CdSiAS_2$ shown in Fig. 1 (b). VBM and CBM also coincide at the Γ point, the material is predicted to be a semiconductor with an energy band gap valence of 0.88 eV, which again is in good agreement with experimental value of 1.55 eV [33]. In Fig. 1 (a), the valence band is sub-divided into nine subbands as seen from the M and A high symmetric line. The valence band width is about 53 eV. The sub bands from -47.5 eV to 53 eV are localized with very flat bands. These sub bands are separated from the subbands in the vicinity of the VBM by a large energy gap of 36.5 eV. Fig. 1 (a) also reveals that the other high symmetry point are possible transition points, this is indicated by the dispersion of the topmost valence band. Also for Fig. 1 (b), one can see a subdivision of the valence band into seven subbands. There is just one subband at the bottom of the valence band which is separated from the top valence band by an energy gap of 23.5 eV. The valence bandwidth is about 37.5 eV.

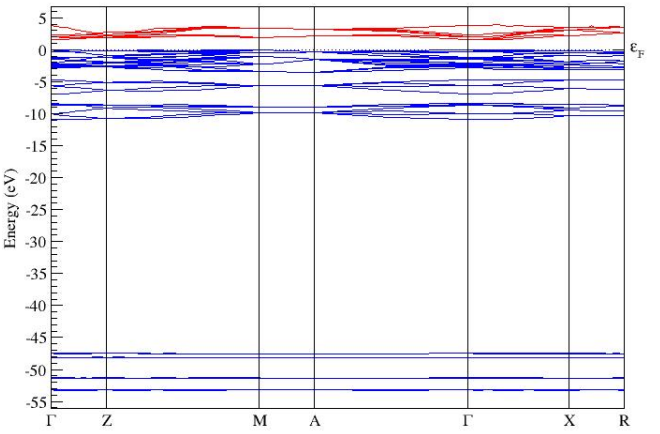

(a)

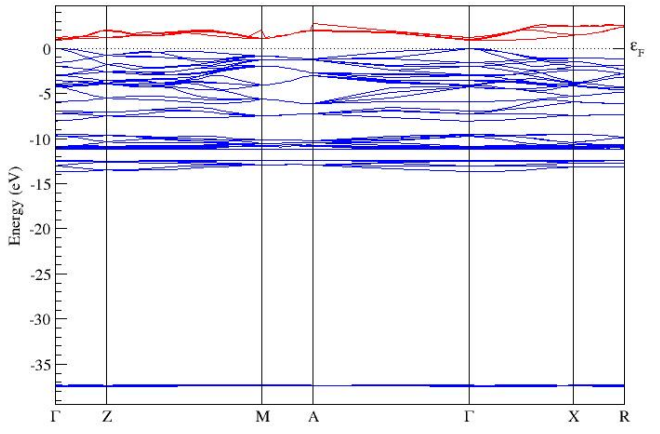

(b)

Fig. 1 The electronic band structure of (a) $CdSiP_2$, (b) $CdSiAs_2$.

The total density of states (TDOS) for $CdSiP_2$ and $CdSiAS_2$ are presented in Figs. 2 (a) and (b), respectively. The TDOS shows the contribution of all the orbitals included in the band structure computations. For $CdSiP_2$ whose TDOS is shown in Fig. 2 (a), the included orbitals are Cd-4d, Cd-5s, P-3p, P-3s, 5i-3p, and Si-3s. These states are represented by the spreads and peaks in the plot. The Fermi level is at 0.1 Ha. Fig. 2 (a) is a

good representation of the band structure of $CdSiP_2$. Fig. 2 (b) displays the TDOS of $CdSiAS_2$, this agrees well with the band structure of $CdSiAs_2$, the included states in the calculation are Cd-4d, Cd-5s, P-3p, P-3s, As-3d, As-4p and As-4s.

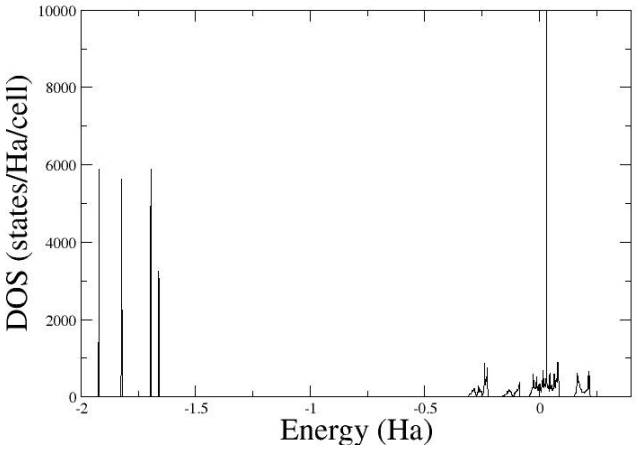

(a)

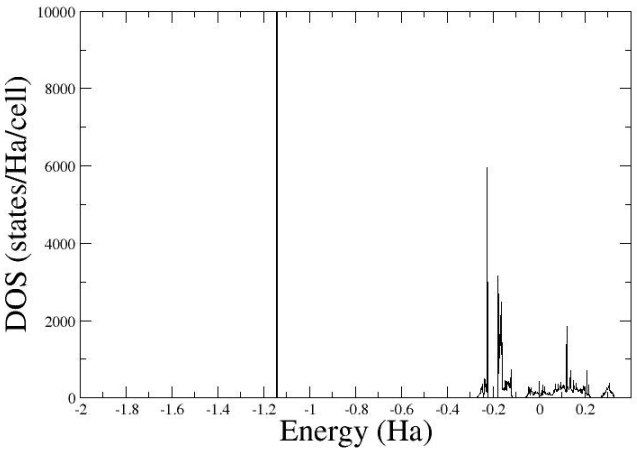

(b)

Fig. 2 The TDOS DOS for (a) $CdSiP_2$, (b) $CdSiAs_2$

The partial density of states (PDOS) for the $CdSiP_2$ are presented for cadmium (Cd), Silicon (Si) and Phosphorus (P) in Figs. 3, 4 and 5 respectively. Fig. 3 displays the orbital contributions of Cd-4d and Cd-5s to the density of states. The curves and peaks in red are the Cd-5s orbital while the ones on black represent Cd-4d states. There is an overlap of the Cd-4d and Cd-5s in the conduction band. There is some form of hybridization involving the Cd-4d with the unoccupied Cd-5p orbitals. The bottom of the conduction band is Cd-4d dominant as well as the top of the valence band. This is clearly seen in Fig. 3. Just like in the conduction band, there is equally an overlap of bottom orbital in the valence band. The narrow peaks at -1.68Ha, -1.7Ha, -1.82Ha and -1.92Ha are of the Cd-4d orbitals. There are other smaller peaks at -1.0 and between -0.3 to -0.2 that also indicate overlap of both orbitals.

Fig. 4 presents the contribution of the Si atom to the TDOS. The bottom of the conduction band is mostly Si-3s with some level of overlap from the Si-3p state. The valence band in the vicinity of the Fermi level are mostly Si-3p. The higher part of the valence band is of Si-3s state.

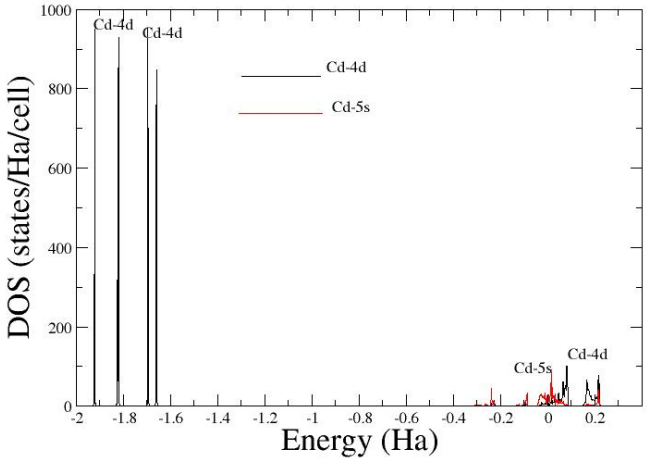

Fig. 3 The PDOS for Cd-4d and Cd-5s orbitals in $CdSiP_2$

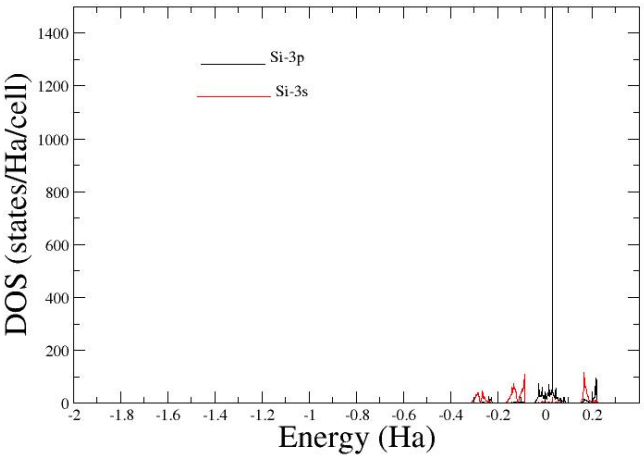

Fig. 4 The PDOS for Si-3s and Si-3p in $CdSiP_2$

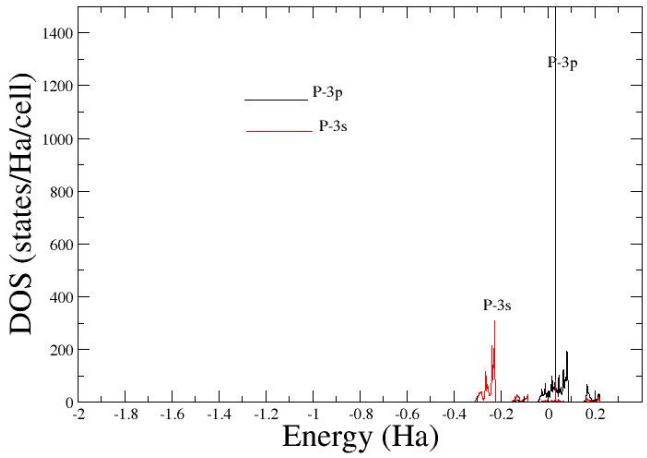

Fig. 5 The PDOS for P-3s and P-3p $CdSiP_2$

The orbital contribution from phosphorus (P) is shown in Fig. 5. The P-3p orbital makes up most of the valence and

conduction band. The peak at -0.22 HA is of the P-3s states.

For $CdSiAs_2$, the PDOS for the atoms Cd, Si and As are presented in Figs. 6, 7 and 8 respectively. The orbital contribution from Cd is presented in Fig. 6, the plot is DOS against energy. The contributions of Cd-4d and Cd-5s orbitals are shown. The states in the energy range 0.0 Ha to about 0.2 Ha are predominantly the Cd-5s state. There is a peak at the top of the valence band at 0.2Ha. This peak is of Cd-4d. The peaks from about -0.22 Ha to – 0.1 Ha are mostly of the Cd-4d states.

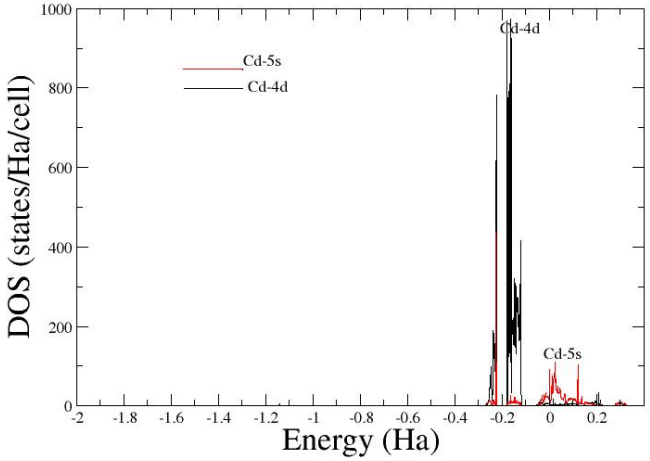

Fig. 6 The PDOS for Cd-4d and Cd-5s orbitals in $CdSiAs_2$

Fig. 7 presents the contribution of the Si-3s and Si-3p orbitals to the TDOS. The Si-3s and Si-3p orbitals overlap in the conduction band, with Si-3s being dominant. The Si-3p orbital is the dominant state in the valence band. The hinder part of the valence band is mostly of the Si-3s orbital. The peaks about -0.05 Ha and 0.0 Ha are of Si-3s. The other peaks between -0.2 and -0.1Hai and -3.0 and -0.2Ha show an overlap of both states. There is a sharp peak of Si-3p at about -0.22Ha.

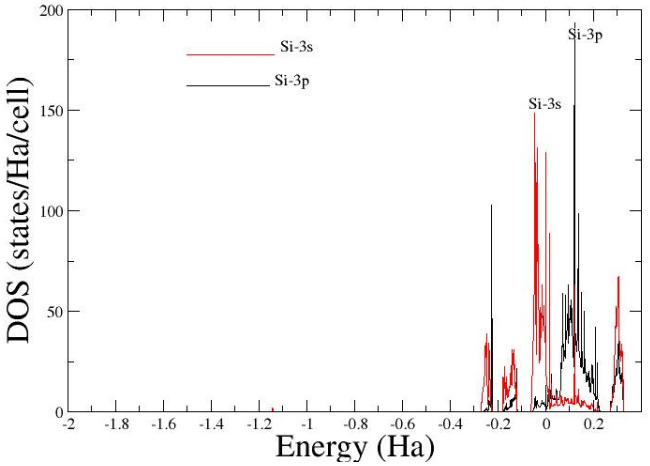

Fig. 7 The PDOS for Si-3s and Si-3p orbitals in $CdSiAs_2$

Fig. 8 shows the contribution from As-3d, As-4p, and As-4s. The conduction band is an overlap of the three Arsenic orbitals with As-4p being the dominant. Most of the valence band is of the As-4p states with a small portion of the As-4s state. The states between -3.0Ha to -0.1Ha are dominantly of the As-4s state. The As-3d state is the narrow peak at -1.14 Ha.

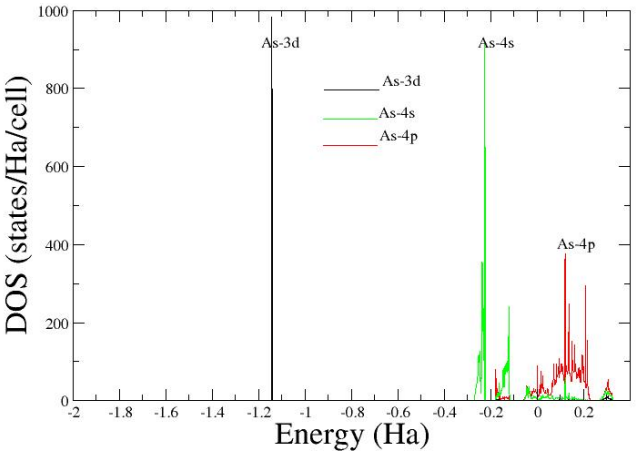

Fig. 8 The PDOS for As-3d, As-3s, and Si-3p orbitals in $CdSiAs_2$

IV. Optical Properties

The dielectric function $\varepsilon(\omega)$ describes how a material response to photonic energy. The dielectric function is a complex function expressed as $\varepsilon(\omega) = \varepsilon_1(\omega) + i\varepsilon_2(\omega)$ where $\varepsilon_1(\omega)$ is the real part and $\varepsilon_2(\omega)$ is the imaginary part. The refractive index of a material is determined by the real part of the materials dielectric functions while its imaginary part determines the materials absorption coefficient. The complex dielectric function plot against energy (frequency) for $CdSiP_2$ is shown in Fig. 9. The real and imaginary dielectric function plots for $CdSiP_2$ are shown in Figs. 9 (a) and (b), respectively. The plots are made up of peaks that show electron transition from valence to conduction band. These transition points are called critical point in the electronic bands of the material. For $CdSiP_2$, Fig. 9 (a) shows some of these critical points. The onset of the first peak indicates the energy band gap, in this case, no scissor shift was applied. The onset of the first peak is at 1.0 eV, the second is at 1.25 eV. There are two higher peaks at 1.5 eV and 2.0 eV. the energy window of the crest is from 1.0 eV to where $\varepsilon_1(\omega)$ falls to -8, this corresponds to 4.75 eV. There is a rapid descend of $\varepsilon_1(\omega)$ as the energy increases. Along this descend are peaks that can be described as humps at 3.0ev, between 3.75 eV and 4.0 eV, and between 4.25 eV and 4.5 eV. The highest peak corresponded to 24 of the dielectric function axis. The plot shows an $\varepsilon_1(0)$ value of 10. The highest peak corresponds to an energy of 1.5 eV.

The imaginary part is presented in Fig. 9 (b). Again, here, the onset of the first corresponds to the energy band gap. The first two small peaks are about 1.1 eV and 1.3 eV. There are several peaks at the crest. Along the ascents of the crest, there is a twin shoulder at about 1.75 eV. There are peaks at the top of the crest at 2.0 eV, 2.25 eV, 2.5 eV, 3.5 eV. The highest peak is at 4.0 eV and corresponds to an $\varepsilon_2(\omega)$ value of 21. The whole energy range is from 0.0 to about 8.25 eV.

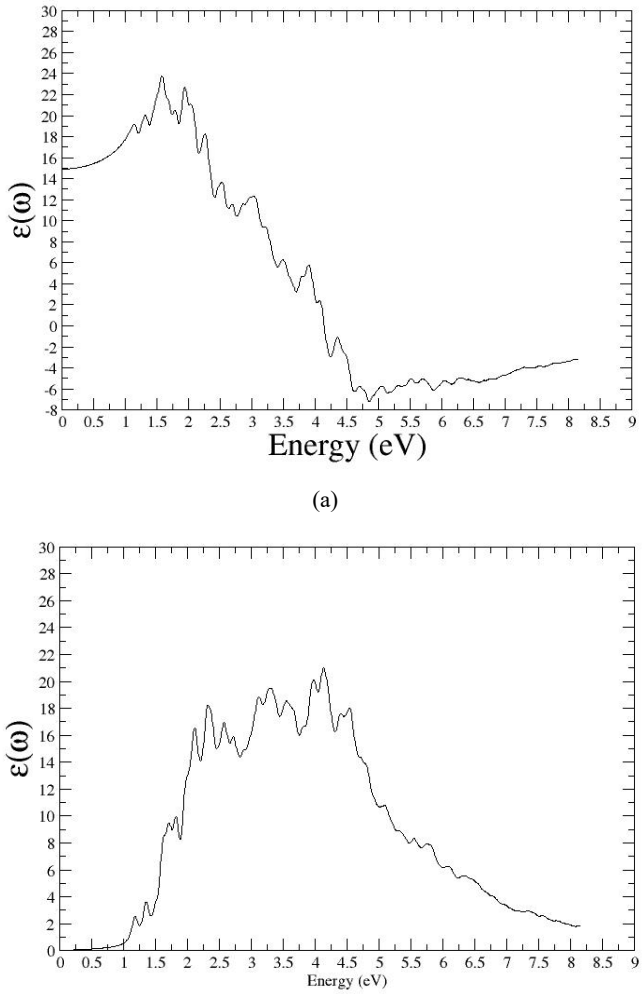

Fig. 9 The dielectric function $\varepsilon^{yy}(\omega)$ of $CdSiP_2$ (a) real part $\varepsilon_1(\omega)$, (b) imaginary part $\varepsilon_2(\omega)$.

From $CdSiAS_2$, the real and imaginary dielectric function plots are presented in Figs. 10 (a) and (b), respectively. Fig. 10 (a) shows two major high peaks at 1.5 eV and 2.0 eV. These peaks correspond to 24 on the ε_2 axis. The peak onset is a small peak at 1.0 eV. There are about five little peaks as the curve descend at increasing energy. There is a distinct peak at 3.5 eV surrounded by three small humps.

There is a low peak at the foot of the curve at 4.75 eV. Also, beyond 5.5 eV are some humps. The calculated value of $\varepsilon_1(0)$ as deduced from Fig. 10 (a) is about 14.9. Fig. 10 (b) shows the onset of transition at 1.0 eV and the first peak is small and it is at 1.25 eV. On the descent of the curve, there is a peak lying between 1.5 eV and 1.75 eV. There are several small peaks, but the highest peak corresponds to 25 on the $\varepsilon_2(\omega)$ axis.

V. Conclusion

The electronic and optical properties of $CdSiP_2$ and $CdsiAs_2$ was computed using the DFT+U method. The calculation showed that both materials are semiconductors with energy band gap of 1.55 eV and 0.88 eV for $CdSiP_2$ and $CdsiAs_2$ respectively. The partial density of states showed that conduction band of $CdSiP_2$ are mostly of the Si-3p, Si-3s and Cd-4d states, while the top of the valence band is predominantly of the P-3p states. For $CdsiAs_2$ the conduction band is composed mostly of the Si-3p, As-4p, and As-4s states. The valence band is predominantly of the As-4p states.

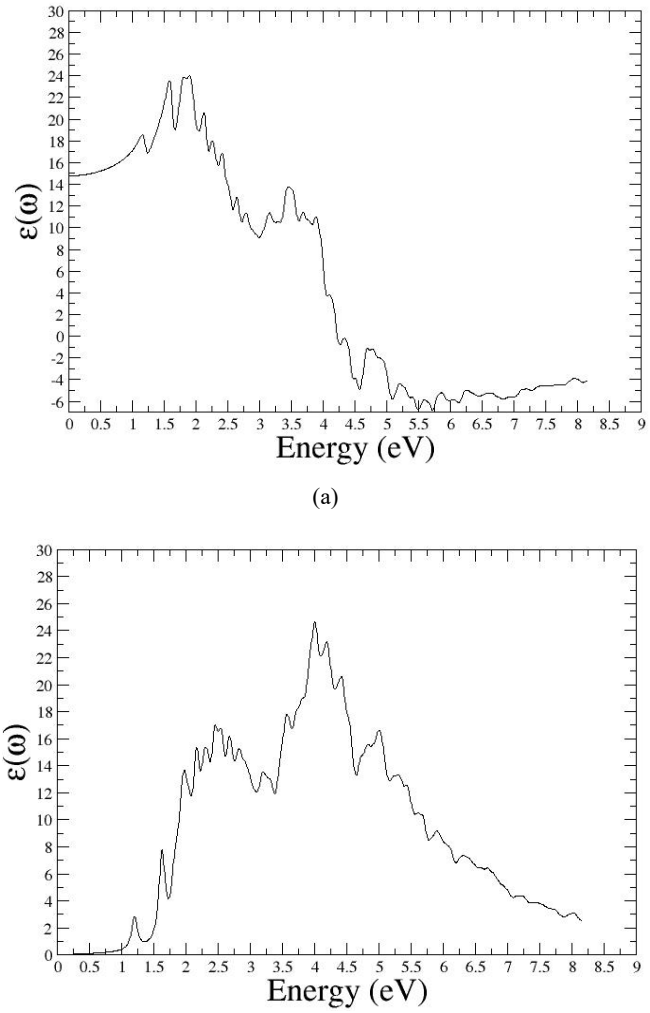

Fig. 10 The dielectric function $\varepsilon^{yy}(\omega)$ of $CdSiAs_2$ (a) real part $\varepsilon_1(\omega)$, (b) imaginary part $\varepsilon_2(\omega)$

References

[1] Ferdinandus, M.R., Gengler, J.J., Averett, K.L., Zawilski, K.T., Schunemann, P.G. and Liebig, C.M., "*Nonlinear optical Measurements of $CdSiP_2$ at near and mid-infrared wavelength,"* Opt. Mater. Express 10, 2066-2074, 2020.

[2] Peremans, A., Lis, D., Cerchet, F., Schunemann, P.G., Zawilski, K.J. and Petrov, V., "Synchronously pumped at 1064nm OPO based on $CdSiP_2$ for generation of high-power picosecond pulses in the mid-infrared near 6.6nm" Proc. SPIE 7582, Nonlinear Frequency Generation and Conversion: Materials, Devices and Applications IX, 75820G. *Nonlinear optical materials with applications in near and mid-112 region of the electromagnetic spectral,* 17 Feb., 2010.

[3] Murtaza, G., Sibghat-Ullah, Khenata, R., Reshak, A.H. and Hayat, S.S., "Optoelectronic properties of $XYAS_2$ (X = Zn, Cd; Y = Si, Sn) Chalcopyrite compound," *J. optoelectronics and Advances Mater.* Vol. 16, No. 1-2, pp. 110-116, 2014.

[4] Shay, J.L and Wernick, J.H., Ternary chalcopyrite semiconductors: Growth, electronic properties and Applications, pergamon press, oxford, 1975.

[5] Isomura, S. and Masumoto, K., "Some optical properties of $ZnGeP_2$ and $CdSiP_2$. $CdSiP_2$ was grown in Sn metal bath," *Phys. Stat. Sol*. (a) 6, k139, 1971.

[6] Kaufmann, U., Schneider, J. and Rauber, A., "ESR detection of antistite lettice defects in Gap, $CdSiP_2$ and $ZnGeP_2$. Nonlinear optical measurements of $CdSiP_2$ at near and mid-infrared wavelengths," *Appl. Phys. Lett.,* 29, 312-313, Issue 5, 312, 1976.

[7] Mughal, S.A., Payne, A.J. and Ray, B., "Preparation and phase studies of the ternary semiconducting compounds $ZnSnP_2$, ZnGeP2, $ZnSiP_2$, $CdGeP_2$ and $CdSiP_2$," *J. Mater. Sci,* 4, 895-901, 1969.

[8] Schunemann, P.G., Zawilski, K.T., Pollak, T.M., Zelmon, D.E., Fernilius, N.C., and Itopkins, F.K., "New Mid-IR Nonlinear Optical Crystal: *conference on Lasers and Electro-optics and 20087 Conference on Quantum Electronics and Laser Science,"* San Jose, CA, USA, Pp. 1-2, 2008.

[9] Petrov, V., Nockk, F., Tunchev, I., Schunemann, P., and Zawilske, K., "Nonlinear Coefficient d_{36} of $CdSiP_2$, Proc of SPIE, Vol. 7197, 71970M, 2009.

[10] Soorinyagoda, R., Piyathilaka, H.P., Zawilski, K.T., Schunemann, P.G. and Bristow, A.D., "Carrier transport and electron-lattice interactions of nonlinear optical crystal $CdGeP_2$, $ZnGeP_2$ and $CdSiP_2$," Arxiv: 2009-04605, 2009.

[11] Zawilski, K.T., Schunemann, P.G., Pollak, T.C., Zelmon, D.E., Fernelius, N.C. and Kenneth, Hopkin, F., "Growth and characterization of large $CdSiP_2$ single crystals," *J. Cryst. Growth,* Vol. 312, Issue 8, Pp. 1127-1132, 2010.

[12] Hui, Y., Shifu, Z., Beijun, Z., Zhiyu, H., Baojun, C. and Shenling, "Differential Thermal Analysis and Crystal Growth of $CdSiP_2$," Rare Metal Materials and Engineering, Vol. 44, Issue 11, Nov. 2015, Pp. 2665-2669, 2015.

[13] Wei, J., Murray, J.M., Hopkins, F.K., Krein, D.M., Zawilski, K.T., Schunemann, P.G. and Guha, S., "Measurement of refractive indices of $CdSiP_2$ at temperature from 90 to 450k*,"* Opt. Mater. Express, Vo. 8, Issue 2, Pp. 235-244, 2018.

[14] Scherrer, E.M., Halliburton, L.E., Golden, E.m., Zawiski, K.T., Schunemann, P.G. and Hopkins, F.K., "*Electron paramagnetic resonance and optical absorption study of acceptors in $CdSiP_2$ crystals,"* AIP Advances 8, 095014, 2018.

[15] Komandin, G.A., Chuchupal, S.V., Goncharov, Y.G., Porodinkov, O.E., Spektor, I.E., Zawilski, K.T. and Schunemann, P.G., "The optical characteristics of the nonlinear optical single crystal $CdSiP_2$ in the terahertz and infrared rangers," *Mater. Res.* Express 6, 026204, 2018.

[16] Bereznaya, S.A., Korotchenko, Z.V., Sarkisov, S.Y., Koroikov, I.V., Kuchumov, B.M., Saprykin, A.I. and Atuchin, V.V., "*Synthesis and characteristics of polycrystalline $CdSiP_2$,"* Mater. Res. Express, Vol. 5(5), 2018.

[17] Li, Y., Huang, J., Huanf, Z., Zbang, G., Gao, Y. and Shi, Y., "Tunable and coherent terahertz source based on CdSiP2 crystal via collinear difference frequency generation," Opt. Let. 47, 2378-2381, 2002.

[18] Carnio, B.N., Zawilski, K.T., Schunemann, P.G., Moutanabbir, O. and Elezzabi, A.Y., "$CdSiP_2$: An emerging crystal for electro-optic sampling from terahertz to the infrared," *Appl. Opt. Mater.* 1, 5, 997-1003, 2023.

[19] Chiker, F., Abbar, B. Tadjei, A., Aourag, H. and Khelifa, B., "Full potential calculations of structural, electronic and optical properties of $CdGeP_2$ and $CdSiP_2$," *CODEN MSBTEK*, Vol. 98(2); Pp. 81-88, 2003.

[20] Basalaev, Y., Gordientko, A.B. and Poplavnoi, A., "Electronic structure of triple phosphids $MgSiP_2$, $ZnSiP_2$ and $CdSiP_2$," *Russ. Phys. J.*, 48(1): 78-83, 2005.

[21] Xiao, J., He, Z., Zhu, S., Chen, B., and Jiang, G., "Hybrid functional study of structural, electronic, bonding and optical properties of CdSiP2," *Comput. Mater.* Vol. 117, Pp. 472-477, May 2016,

[22] Hou, H.J., Zhu, H.J., Xu, J., Zhang, S.R. and Xie, L.H., "Structural, Elastic and Optical properties of Chalcopyrite $CdSiP_2$ with the Application in Nonlinear Optical from First Principle Calculations," *Braz. J, Phys,* Vol. 46, Issue 6, Pp. 628-635, 2016.

[23] Hadda, T., Baaziz, H., Ghellab, T. and Zoulikha, C., "Calculations of the structural, electronic, optical, and elastic parameters of $CdSiX_2$ (X = P, AS) compounds based on first principle theory," *Physical Status Solidi (b).* 259 (11), 2022.

[24] Jabbar, O. and Reshak, A.H., "Structural, electronic and optoelectronic properties of XYZ_2 (X = Zn, Cd; Y = Si, Sn; Z = Pnicogens). Calcoprite compounds: First principle calculations," Exp. Theo. *NANOTECHNOLOGY* 7, 97-110, 2023.

[25] Yu, Y., Shen, Y.H., Kong, X.G., Zeng, T.X. and Deng, J., "Structural, electronic, optical and vibrational properties of $CdSiP_2$ from first principles," *Solid State Communications*, 115283, 2023.

[26] Kumavat, S., Nambakkat, L., Jain, R. and Chandra A.R., "First principles study of $CdSiAS_2$ semiconductor compound: Bulk, (100) and (001) surfaces," *AIP conference proceedings,* 2105(1): 020009, May 2019.

[27] Kumavat, S., Lakshmi, N., Jain, R., Jain, V. and Chandra, A.R., "Electronic and optical properties of $CdSiAS_2$ semiconductor compound," Mater. today, Proc, Vol. 47, Part 18. Pp. 6504-6507, 2021.

[28] Kimmel, A., Lux-Steiner, M., Klein, A. and Bucher, E., "Single crystal growth of p-Doped $CdSiAS_2$. Chemical vapour transport using cadmium chloride as the agent of transport," SLAC Pub 4603, 1998.

[29] Avirovic, M., Lux-Steiner, M., Elrod, U., Honigschmid, J. and Bucher, E., "Single crystal growth of $CdSiAS_2$ by chemical vapour transport; its structure and electrical properties," *J. cryst. growth*, Vol. 67, Issue 2, Pp. 185-194, 1984.

[30] Osinsky, A., chernyak, L., Temkin, H., Wen, Y.C. and Parkinson, B.A., "Effect of surphur doping on optical anisotropy of $CdSiAS_2$," *Appl. Phys. Lett.* 69, 2867-2869, 1996.

[31] Gonze X., Beuken J.-M., Caracas R., Detraux F., Fuchs M., Rignanese G.-M., Sindic L., Verstraete M., Zerah G., Jollet F., Torrent M., Roy A., Mikami M., Ghosez Ph., Raty J.-Y., and Allan D.C., "First-principles computation of material properties: the Abinit software project," Comput. Mater. Sci. 25, 478-492, 2002.

[32] Gonze X., Rignanese G.-M., Verstraete M., Beuken J.-M., Pouillon Y., Caracas R., Jollet F., Torrent M., Zerah G., Mikami M., Ghosez Ph., Veithen M., Raty J.-Y., Olevano V., Bruneval F., Reining L., Godby R., Onida G., Hamann D. R., and Allan D. C., "A brief Introduction to the Abinit software package," Z. Kristallogr. 220, 558-562, 2005.

[33] Madelung O., Semiconductors: Data Hand book, Springer, 3rd edition, 2004.